Kálmán and Domokos *EPJ Quantum Technology* (2020) 7:2
https://doi.org/10.1140/epjqt/s40507-020-0078-7

EPJ Quantum Technology
a SpringerOpen Journal

RESEARCH Open Access

Sensing microwave photons with a Bose–Einstein condensate

Orsolya Kálmán[1]* and Peter Domokos[1]

*Correspondence:
kalman.orsolya@wigner.mta.hu
[1]Department of Quantum Optics and Quantum Information, Institute for Solid State Physics and Optics, Wigner Research Centre for Physics, Budapest, Hungary

Abstract

We consider the interaction of a magnetically trapped Bose–Einstein condensate of Rubidium atoms with the stationary microwave radiation field sustained by a coplanar waveguide resonator. This coupling allows for the measurement of the magnetic field of the resonator by means of counting the atoms that fall out of the condensate due to hyperfine transitions to non-trapped states. We determine the quantum efficiency of this detection scheme and show that weak microwave fields at the single-photon level can be sensed.

Keywords: Bose–Einstein condensate; Waveguide resonator; Magnetic field sensing; Hyperfine transition; Atomlaser

1 Introduction

Sensing extreme low-intensity radiation fields in the quantum regime requires high-efficiency, low-noise detectors. In the case of the optical wavelength range, single-photon detectors are widely available. The thermal radiation at optical frequencies is naturally suppressed at room temperature. Moreover, the electric dipole transitions in atoms or in semiconductors give rise to large coupling to the electromagnetic field and, ultimately, to high quantum efficiency. By contrast to the optical case, photon counting of microwave radiation is still a formidable task. It is possible to count microwave photons of a resonator, for example, by means of Ramsey interferometry with highly-excited circular Rydberg atoms [1]. Analogous schemes have been demonstrated for microwave waveguide resonators integrated in a circuit with strongly coupled superconducting non-linear elements [2–7]. In these chip-based circuits the quantization of flux and charge leads to quantized electric and magnetic fields at microwave frequencies, in accordance with the longitudinal dimension of the device [8].

There are approaches to photon detection, in the microwave frequency regime too, which are based on the same principle as that of commonly used optical detectors, i.e., the absorption by a ground-state material probe. In this regime, the naturally occurring transitions in material quantum systems are magnetic ones, which are weaker than the electric dipole transitions typically by a factor of the fine structure constant $\alpha = 1/137$. One promising candidate is the spin degree of freedom of point defects in nanocrystals,

which provides for a portable, well localised probe of the field [9, 10]. Alternatively, hyperfine transitions of atoms in the electronic ground state can be considered [11]. In this approach, the quantum efficiency of the detection can benefit from the collective enhancement gained by using a degenerate atomic cloud, i.e., a Bose–Einstein condensate (BEC) of trapped atoms. The price to pay is that the condensate is not so well localised as a single spin or atom, nevertheless, it is still orders of magnitude smaller than the corresponding wavelength of the radiation. The trapped BEC is an ideal probe of weak external fields due to the fact that all their relevant degrees of freedom can be controlled with unprecedented precision [12, 13]. That is, it approaches closely the ultimate quantum-noise limit requested from a detector.

In this paper we evaluate the detection capabilities of a BEC in the microwave regime. In particular, we investigate whether a microwave field at the single-photon level can be sensed and translated to a detectable signal by means of the atomlaser scheme [14, 15] for magnetic noise measurement [16–18]. It has been first proposed in Ref. [19] that strong-coupling between ultracold atoms and the magnetic field of a waveguide resonator can be achieved. Recently, the near-field microwave radiation of a coplanar waveguide resonator (CPW) has been successfully coupled to ultracold atoms [20]. In this experiment the light-shift of a hyperfine transition induced by the strongly driven resonator mode in the large photon number regime was detected by Ramsey interferometry and the possibility of coherent control of the hyperfine states was demonstrated by directly observing resonant Rabi oscillations. Here we consider the opposite, weak field limit and restrict our aim at the detection of a feeble radiation field. To this end, we resort to the atomlaser detection method which relies on counting single atoms outcoupled by the measured field and falling out of the trap due to gravity [14, 18].

The paper is organized as follows. In Sect. 2 we consider a setup where the condensate is situated at the antinode of the microwave magnetic field under the microwave resonator, so that the outcoupled atoms can fall out of the trap due to gravity. Section 2.1 is devoted to the description of the detection scheme. Section 2.2 overviews the geometry and the description of the coplanar waveguide resonator. In Sect. 3 we consider the process of sensing the magnetic field of a single photon in the resonator. First, we give an approximation for the magnetic field when there is, on average, a single photon in the resonator, and present an analytical formula for the number of outcoupled atoms. Then, in Sect. 4 we consider typical parameters for the BEC and the CPW for the proposed setup and estimate how many outcoupled atoms would be found per a single microwave photon in a given detection volume assuming perfect ionization detection of the atoms. We conclude in Sect. 5.

2 The setup

The principle of the detection relies on the continuous atomlaser scheme [18]. Atoms are localised in a static magnetic trap and are prepared in a Bose–Einstein condensate in a given hyperfine state. Photon absorption from a driving microwave field leads to resonant hyperfine transitions from the trapped to an untrapped state of the atoms. Counting the outcoupled atoms [21], once spatially separated from the trap, characterises the strength of the magnetic field component of the microwave radiation field and gives information on the photon number. A possible geometry is sketched in Fig. 1. In order to enhance the coupling, we consider the near-field of a microwave coplanar waveguide resonator as a source of the radiation field.

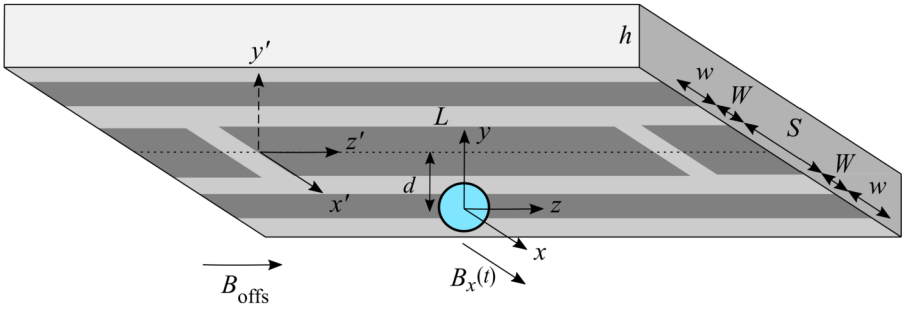

Figure 1 Setup. Sketch of the setup to sense the magnetic field of a CPW with a BEC. The ultracold atom cloud is situated at the center of the central conductor of the waveguide resonator. The geometry of the CPW ensures that its magnetic field is polarized in the x direction at the location of the BEC. The magnetic field $B_x(t)$ of the CPW oscillates in time with an angular frequency of ω_{CPW} that is resonant with a magnetic dipole transition of the BEC atoms, and induces transitions from the trapped state into an untrapped one

2.1 The Bose–Einstein condensate

We consider ultracold ^{87}Rb atoms prepared in the hyperfine manifold $F = 2$ of the ground state $5^2S_{1/2}$, placed in an external magnetic field $\mathbf{B}(\mathbf{r})$ in the presence of gravity. The total atomic angular momentum $\hat{\mathbf{F}}$ interacts with the magnetic field according to the Zeeman term $H_Z = g_F\mu_B\hat{\mathbf{F}}\mathbf{B}(\mathbf{r})$, where $\mu_B = e\hbar/2m_e$ is the Bohr magneton, g_F is the Landé factor, and $\hat{\mathbf{F}}$ is measured in units of $\hbar$. The dominant component of the magnetic field $\mathbf{B}(\mathbf{r})$ is a homogeneous offset field B_{offs} pointing along the z direction. The eigenstates of the spin component $\hat{F}_z$, labelled by $m_F = -2, -1, 0, 1, 2$, are well separated by the Zeeman shift $\hbar\omega_0 = \mu_B B_{\text{offs}}/2$ (see Fig. 2), the $m_F = 2$ level being the highest in energy (due to the fact that $g_{F=2} = 1/2$). The inhomogeneous component of the magnetic field $\mathbf{B}(\mathbf{r})$ creates a harmonic trapping potential $V_T(\mathbf{r}) = \frac{M}{2}[\omega_x^2x^2 + \omega_y^2y^2 + \omega_z^2z^2]$ around the minimum of the total magnetic field in which we assume atoms to be confined in the low-field seeking state $|2,1\rangle$. Here ω_x, ω_y and ω_z are the trap frequencies in the x, y, and z directions, respectively, and M is the atomic mass. In the presence of gravity, the atoms are still under the effect of an effective harmonic trapping potential $V_T^{\text{eff}}(\mathbf{r}) = V_T(\mathbf{r}) + Mgy = \frac{M}{2}[\omega_x^2x^2 + \omega_y^2(y + g/\omega_y^2)^2 + \omega_z^2z^2] - Mg^2/2\omega_y^2$, where g is the gravitational acceleration. As a result, the trapped atomic cloud is displaced from the minimum of the magnetic field into the minimum of this effective potential, $-g/\omega_y^2$, which is the so-called gravitational sag.

The homogeneous offset magnetic field splits the magnetic sublevels of the $F = 1$ manifold as well (see Fig. 2), the splitting between consecutive levels also being $\hbar\omega_0$ (here the $m_F = -1$ level is the highest in energy as $g_{F=1} = -1/2$). As the untrapped state of the atoms, we select the state $|1,0\rangle$, as it is insensitive to the offset and trapping magnetic fields, and atoms in this state simply fall out of the trap due to gravity. In our setup in Fig. 1 we assume that the dominant component of the CPW's magnetic field is $B_x(t)$ (cf. Sect. 2.2). $B_x(t)$ is orthogonal to B_{offs} and oscillates in time with an angular frequency of ω_{CPW}, thus, it can induce transitions between the trapped hyperfine state $|2,1\rangle$ and the untrapped $|1,0\rangle$ state (as indicated by the green arrow in Fig. 2). We note that there are other possible hyperfine transitions in the ground state manifolds, with a trappable inital state and an untrapped final state, as discussed in Appendix A. Our choice is motivated by the fact that the untrapped state $|1,0\rangle$ can fall out of the cloud below the trap due to gravity and is therefore more easily detectable by atom counting techniques, than a state that is repulsed by the trapping magnetic field.

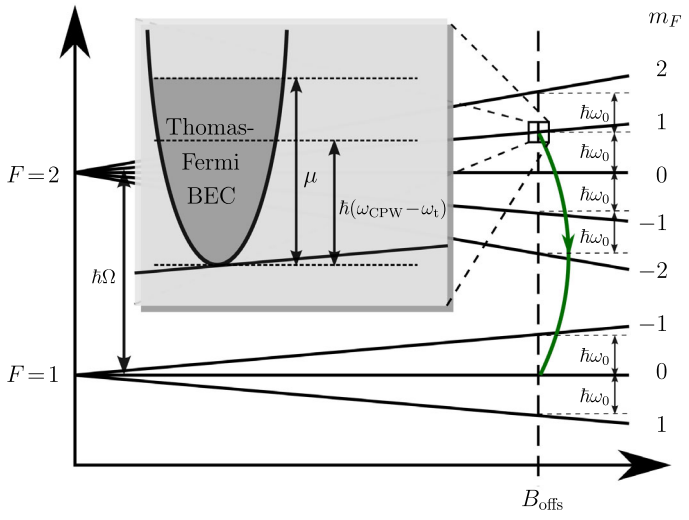

Figure 2 Level scheme of ^{87}Rb. The Zeeman splitting of the $5^2S_{1/2}$ ground state of ^{87}Rb, the harmonic trapping potential for the atoms in the state $F = 2, m_F = 1$, and the different frequencies involved in the process

In the mathematical description it is convenient to choose the origin of the y axis such that the single-particle potential for the atoms in state $|1,0\rangle$ be given by $V_{|1,0\rangle} = Mgy$, corresponding to the fact that the origin coincides with the center of the atomic cloud. Then the total single-particle potential affecting the trapped atomic state is given by $V_{|2,1\rangle}(\mathbf{r}) = \hbar\omega_{\rm t} + V_{\rm T}(\mathbf{r})$, where $\omega_{\rm t} = \Omega + \omega_0 + \frac{Mg^2}{2\hbar\omega_y^2}$ is the transition frequency at the center of the cloud in the presence of gravity, $\Omega = 2A_{\rm hfs} \approx 2\pi \times 6.8347$ GHz being the hyperfine splitting of the $5^2S_{1/2}$ state, and $V_{\rm T}(\mathbf{r})$ is the harmonic part of $V_{\rm T}^{\rm eff}$ in the transformed coordinate system which now has the same form as the trapping potential without gravity.

In the magnetically trapped $|2,1\rangle$ state, we assume a pure Bose–Einstein condensate (BEC) described by the second-quantized field operator $\hat{\Psi}_{|2,1\rangle}(\mathbf{r},t) = \sqrt{N_0}\Phi_{\rm BEC}(\mathbf{r}) \times e^{-i(\omega_{\rm t}+\mu/\hbar)t}$, where the wavefunction $\Phi_{\rm BEC}$ is the stationary solution of the Gross–Pitaevskii equation with chemical potential μ and atom number N_0. Atoms in the state $|1,0\rangle$, which can be described by the field operator $\hat{\Psi}_{|1,0\rangle}(\mathbf{r},t)$ are only affected by gravity and, due to collisions with the condensate atoms, by the influence of the mean-field potential $N_0 g_s \Phi_{\rm BEC}^2(\mathbf{r})$, with $g_s = 4\pi\hbar^2 a_s/M$, and scattering length a_s ($a_s = 5.4$ nm for ^{87}Rb).

We consider a setup where at the location of the BEC the microwave magnetic field is quasi-homogeneous in the x direction, and oscillates in time with a frequency of $\omega_{\rm CPW}$, i.e., $B_x(t) = B_x\cos(\omega_{\rm CPW}t)$. As discussed in Appendix A, in our case, it is the electron spin magnetic moment which determines the coupling of the atomic magnetic moment with this magnetic field, so that the corresponding perturbation can be written as $V_I = g_S\mu_{\rm B}B_x(t)\hat{S}_x$, where $\hat{S}_x = (\hat{S}_+ + \hat{S}_-)/2$, S_x being the x component of the electron spin operator, with S_+ and S_- the spin raising and lowering operators. We assume that initially no atoms populate the $|1,0\rangle$ state. To leading order in the small quantum field amplitude $\hat{\Psi}_{|1,0\rangle}$, the equation of motion in rotating-wave approximation reads

$$i\hbar\frac{\partial}{\partial t}\hat{\Psi}_{|1,0\rangle} = \left[-\frac{\hbar^2\nabla^2}{2M} + Mgy + N_0 g_s \Phi_{\rm BEC}^2(\mathbf{r})\right]\hat{\Psi}_{|1,0\rangle} - \hbar\eta\Phi_{\rm BEC}(\mathbf{r})e^{i\Delta\cdot t}, \tag{1}$$

where $\eta = \sqrt{3}\mu_B B_x \sqrt{N_0}/4\sqrt{2}\hbar$ and $\Delta = \omega_{\mathrm{CPW}} - \omega_t - \mu/\hbar$ is the detuning of the microwave frequency from the transition frequency at the center of the atomic cloud. Here we considered the BEC as an undepleted reservoir, i.e., the quantum fluctuation $\delta\hat{\Psi}_{|2,1\rangle}$ was neglected in comparison with Φ_{BEC} as it corresponds to a second-order process. Furthermore, we assumed that the quantum field components in the $|1, m_F \neq 0\rangle$, or the $|2, m_F \neq 1\rangle$ sublevels are also negligible when the $|2,1\rangle \rightarrow |1,0\rangle$ transition is on resonance with the microwave frequency as they are detuned by $\Delta\omega \geq \hbar\omega_0$. Finally, we neglect the transitions $|1,0\rangle \rightarrow |2,1\rangle$ back to the condensate, originating from the matrix element $\langle 2,1|\hat{S}_+|1,0\rangle \neq 0$, because we assume that the atoms fall out of the trap before completing a Rabi cycle. Within these approximations, the dynamics of the outcoupled field $\hat{\Psi}_{|1,0\rangle}(\mathbf{r}, t)$ is decoupled from the other Zeeman states.

The solution to the partial differential equation (1) is outlined in Appendix B. Here we note that the outcoupled atom field $\hat{\Psi}_{|1,0\rangle}$ can be constructed by using plane waves in the horizontal directions, and the solutions of the quantum mechanical free-fall problem, i.e., the Airy functions, in the vertical direction. The absolute square of the outcoupled atom field describes the local density of atoms at a position $\mathbf{r}$, even if the underlying Airy-type of wavefunctions are not normalizable, and, according to Eq. (10) can be expressed as

$$N(\mathbf{r}) = \left\langle \hat{\Psi}^{\dagger}_{|1,0\rangle}(\mathbf{r})\hat{\Psi}_{|1,0\rangle}(\mathbf{r}) \right\rangle = \left(\frac{\hbar\eta}{Mgl_0}\right)^2 D(\mathbf{r}), \tag{2}$$

where $l_0 = (\hbar^2/2M^2g)^{1/3}$ is the natural length of the Airy function. $D(\mathbf{r})$ is a density function in coordinate space with the dimension of 1/volume, and it accounts for the fact that in the outcoupling process the energy of the microwave magnetic field is distributed among the three coordinate directions in the outcoupled atom field. Its value for a given detuning Δ between the frequency of the microwave field and the transition frequency of the atoms inside the cloud, is mainly affected by the overlap between the Airy function and the BEC wave function (the latter being dependent on the geometrical shape of the cloud), and the distance of the spatial location $\mathbf{r}$ from the atomic BEC as can be seen from Eq. (11) and (12). In Ref. [18] it was shown that for a spherical BEC of radius $a \gg l_0$, $D(\mathbf{r})$ is maximum when $\Delta \approx 0$, i.e., when the detuning of the frequency of the outcoupling magnetic field from the transition frequency at the center of the BEC is zero, therefore, in what follows, we will focus on this case.

2.2 Coplanar waveguide resonator

We consider a (superconducting) half-wavelength coplanar waveguide resonator (CPW) of length L with a central conductor strip of width S and two ground electrodes of width w at a distance W from the central conductor situated on a substrate of thickness h and relative permittivity ε_r (see Fig. 1). The electric and magnetic fields of the resonator oscillate in time with a frequency of ω_{CPW}, with their maxima shifted in space: The magnetic field has the largest amplitude at the center of the central conductor, where the electric field is zero, and zero at the two ends, where the electric field has a maximum amplitude. For the amplitude of the components of the magnetic field analytic formulas obtained by the quasistatic approximation are presented in Appendix C. Here we assume that the (half) transversal size of the CPW, $b = S/2 + W + w$, is much smaller than the wavelength $\lambda = 2\pi c/\omega_{\mathrm{CPW}}$ of the microwave field of the cavity (c being the speed of light in vacuum). In

this case, the z component of the magnetic field, $B_z(t)$, can be neglected compared to the other components (see Eq. (13)). $B_x(t)$ may be considered to be the dominant component of the magnetic field around the center of the central conductor, as its amplitude B_x has a cosine shape in the transversal direction, and is maximum at the center. The amplitude of $B_y(t)$, on the other hand, has a sinusoidal dependence on the transversal coordinate, is zero at the center, and grows approximately linearly in the transversal direction in the close neighborhood of the center, where, the amplitude B_x, due to its cosine shape, may be approximated to be constant. In our setup, we assume that the BEC cloud is situated under the center of the CPW (see Fig. 1). Thus, we neglect the effect of $B_y(t)$ on the atoms as well as the inhomogeneity of the amplitude B_x, and approximate the latter with its value at the center of the BEC cloud. These assumptions are plausible as the atom density in the condensate is the largest around the center of the cloud and decreases rapidly in the radial direction.

As we have shown in Sect. 2.1, in order to effectively couple the CPW to the hyperfine transition $|2,1\rangle \rightarrow |1,0\rangle$ of the BEC atoms, the microwave frequency of the resonator should be resonant with the transition frequency of the atoms at the center of the BEC, corresponding to $\Delta = 0$, i.e., $\omega_{\mathrm{CPW}} = \omega_{\mathrm{t}} + \mu/\hbar$. Due to the effect of gravity, the transition frequencies at the top and bottom of the atom cloud are detuned by $-Mga/\hbar$ and $Mga/\hbar$ from ω_{CPW}, respectively, with a being the semi-axis of the condensate in the direction of gravity. As long as the corresponding bandwidth $2Mga/\hbar$ is larger than the linewidth of the CPW resonator mode, the full power spectrum of the field mode contributes to the outcoupling of the atoms. In the case we consider, there is an order of magnitude difference, which justifies the monochromatic approximation which was assumed when we derived Eq. (2).

As the mode wavelength corresponding to ω_{CPW} is given as $\lambda_g = \lambda/\sqrt{\varepsilon_{\mathrm{eff}}} = 2\pi c/(\omega_{\mathrm{CPW}}\sqrt{\varepsilon_{\mathrm{eff}}})$, a CPW of length $L = \lambda_g/2$ is needed. We note that the effective dielectric constant $\varepsilon_{\mathrm{eff}}$ can be aproximated by analytical methods using the conformal mapping technique [22] cf. Appendix D.

3 Results: the quantum efficiency of the sensing process

In the proposed setup the microwave field is generated as a near-field of an externally driven coplanar waveguide resonator. In this geometry, the resonator can significantly enhance the local microwave field strength at the position of the atoms. The photons are transmitted through the waveguide resonator at a rate $\kappa = \omega_{\mathrm{CPW}}/Q$, with Q being the quality factor of the CPW. We will consider the "bad-cavity" regime in which the driving and the transmission loss of photons from the resonator dominates the dynamics due to the coupling to the atoms (see Sect. 4). Therefore, one can safely neglect the back-action of the atomic hyperfine transitions on the CPW mode. The microwave field is in the steady-state set by the driving amplitude. We will assume that the field is in a coherent state with a mean photon number $\langle n_{\mathrm{photon}}\rangle = 1$.

In order to determine the number of outcoupled atoms corresponding to a mean photon number $\langle n_{\mathrm{photon}}\rangle = 1$ in the microwave cavity, we estimate the maximum of the inhomogeneous magnetic field as the field corresponding to a single energy quantum $\hbar\omega_{\mathrm{CPW}}$ in the microwave cavity

$$|B_{\mathrm{max}}| = \sqrt{\frac{2\mu_0\hbar\omega_{\mathrm{CPW}}}{V_c}}, \tag{3}$$

since when the magnetic field is maximal (in time), then all of the photon's energy is carried by the magnetic field, cf. Sect. 2.2. Using Eqs. (13) we can estimate the mode volume $V_c = \int_V d^3\mathbf{r}|\mathbf{B}(\mathbf{r}')|^2/|B_{\max}|^2$ of the CPW cavity to be $V_c \approx Lb^2/\pi$.

Alternatively, one can estimate $|B_{\max}|$ based on the circuit quantum electrodynamical (CQED) formulation [8], where the amplitude of the voltage operator is given by $V_0 = \sqrt{\hbar\omega_{\mathrm{CPW}}/C_{\mathrm{CPW}}}$, with C_{CPW} being the total capacitance of the cavity. Substituting this into Eqs. (13) and using Eq. (20) the maximum of the magnetic field can be written as

$$\left|B_{\max}^{\mathrm{CQED}}\right| = \sqrt{\frac{2}{\kappa_0}} s_1 \sqrt{\frac{2\mu_0\hbar\omega_{\mathrm{CPW}}}{Lb^2}}. \tag{4}$$

We will show that for the physical parameters to be considered in our calculations, the above two estimations are in good agreement.

In order to maximize the coupling between the two systems, the BEC cloud needs to be placed close enough to the surface of the CPW, while avoiding the effect of van der Waals forces on the trapped atoms. The latter can be achieved if the distance d_0 between the BEC and the surface of the CPW is $d_0 \gtrapprox 1$ μm [23, 24]. Then, according to Eqs. (13), at a distance of $d > (d_0 + a)$ in the negative y' direction, i.e., at the center of the BEC ($y = 0$), the magnitude of the magnetic field is decreased by the factor $e^{-d\gamma_1} \approx e^{-\frac{\pi d}{b}}$. Here we assumed that $\gamma_1 \approx \pi/b$, which is valid for $b \ll \lambda$. Therefore, we estimate the amplitude of the magnetic field to be

$$B_x = e^{-\frac{\pi d}{b}}|B_{\max}|. \tag{5}$$

In an experimental situation, the outcoupled atoms can be counted by ionizing a part of the beam of atoms with lasers. This defines a detection volume V_{d}. To get the number of outcoupled atoms in this volume, we need to integrate $N(\mathbf{r})$ of Eq. (2) over V_{d}

$$\mathcal{N} = \frac{N_0}{V_{\mathrm{BEC}}}\left(\frac{\sqrt{15}\mu_B}{8Mgl_0}\right)^2 B_x^2 \int_{V_{\mathrm{d}}} \overline{D(\mathbf{r})}\, d^3\mathbf{r}, \tag{6}$$

where $\overline{D(\mathbf{r})} = D(\mathbf{r})/(\mu/Ng_s)$ is dimensionless and we used the fact that the chemical potential of a condensate can be written as $\mu = 5N_0g_s/(2V_{\mathrm{BEC}})$ in the Thomas–Fermi approximation, where the BEC wave function is given by $\Phi_{\mathrm{BEC}}(\mathbf{r}) = \sqrt{[\mu - V_{\mathrm{T}}(\mathbf{r})]/N_0g_s}$. In the following, we will assume that the ionization detection has unit efficiency, i.e., the number of atoms in the above formula can be considered the detection signal.

4 Discussion: numerical estimation

Let us consider a spherical condensate of radius $a = 5$ μm with $N_0 = 2 \times 10^4$ ^{87}Rb atoms, which corresponds to a trapping frequency $\omega_x = \omega_y = \omega_z = 2\pi \times 84$ Hz and a chemical potential $\mu/\hbar = 2\pi \times 0.75$ kHz. The hyperfine splitting of the atoms is $\Omega \approx 2\pi \times 6.8347$ GHz and in a z-directional offset magnetic field $B_0 = 0.1$ mT the Zeeman splitting of the magnetic sublevels is $\omega_0 = 2\pi \times 0.7$ MHz, and therefore the frequency of the cavity needs to be $\omega_{\mathrm{CPW}} = 2\pi \times 6.8354$ GHz.

We assume that the CPW is constituted by Al-film conductors on a Sapphire substrate ($\varepsilon = 11.5$) with dimensions $S = 15$ μm, $W = 10$ μm, $w = S/2$, $b = 25$ μm, and $h = 500$ μm.

Such CPW's have been measured to have a quality factor of $Q = 1.72 \times 10^6$ for low power, i.e., $\langle n_{\text{photon}} \rangle \approx 1$ [25]. The effective permittivity is determined to be $\varepsilon_{\text{eff}} = 6.25$, and the length of the cavity is $L = 8.778$ mm. Then, with a distance of $d = 7$ μm between the center of the BEC and the CPW, the amplitude of the outcoupling magnetic field can be approximated to be $B_x \approx 2.56$ nT. (Note that for the same parameters, the estimation based on the circuit QED result gives $|B_{\text{max}}^{\text{CQED}}| \approx 2.25$ nT.) This magnetic field yields an outcoupling strength $\eta \approx 10^4 \text{s}^{-1}$. The corresponding Rabi cycle time back to the trapped state $|2,1\rangle$ is then $2\pi/\eta \sim 0.57$ ms, whereas the atom in the untrapped state $|1,0\rangle$ leaves entirely the BEC volume in a period of time 1 ms. As the overlap with the BEC vanishes on the time scale of 1 ms, the initial reduction on a shorter time scale impedes the Rabi precessing between the falling atoms and the BEC. This justifies the approximation of neglecting the transitions $|1,0\rangle \rightarrow |2,1\rangle$ back to the condensate in Eq. (1).

Based on our numerical results applying Eq. (6) (together with Eqs. (11) and (12) for $\Delta = 0$) we find that by choosing the center of the detection volume at $y_c = 65$ μm below the center of the condensate with a height of $y_d = 60$ μm, the number of atoms in this volume is $\mathcal{N} \approx 3$. Assuming ionization detection scheme with efficiency close to 1 [21], all these atoms are detected, and $\mathcal{N} \approx 3$ calibrates the signal of sensing the weak magnetic field corresponding to a stationary coherent state with mean $\langle n_{\text{photon}} \rangle = 1$ in the resonator.

The number of $\mathcal{N}$ atoms in the detection volume is generated in a given duration of time τ, which is the time difference of reaching the upper and lower border of the detection volume, i.e. the heights $y_c \pm y_d/2$. Using the assumed parameters, the detection interval is between 35 μm and 95 μm, which corresponds to a time period of $\tau = 1.7$ ms in free fall. Note that the photon lifetime in the resonator is $\kappa^{-1} = 40$ μs. That is, for the generation of $\mathcal{N} = 3$ atoms, on average, in the presence of the stationary state with $\langle n_{\text{photon}} \rangle = 1$, the necessary time period of $\tau = 1.7$ ms amounts to the transmission of about $\kappa\tau = 42$ photons.

As we can see from these numbers, there is, in principle, no fundamental reason which would inhibit reaching the 100% detection efficiency for single photons enclosed in a high-Q cavity in this scheme. However, the detection scheme with the detection time around 1 ms is relatively 'slow' compared to the recently reported fast detection schemes in circuit QED systems [4–7], where the time scale is in the range of μs.

The value of $\mathcal{N}$ in our setup is mainly affected by the magnitude of the magnetic field, which can be increased by reducing the width W between the center conductor and the ground planes of the CPW, but it would require to move the BEC closer to the cavity, which is also limited by the radius of the cloud. Increasing the number N_0 of trapped atoms with increasing cloud radius does not significantly increase $\mathcal{N}$, as can be seen from Eq. (6). However increasing N_0 while keeping the cloud dimensions the same or enlarging the detection volume can obviously increase the number of outcoupled atoms.

5 Conclusion

We have evaluated the capabilities of a magnetically trapped Bose–Einstein condensate of Rubidium atoms to detect the magnetic field of a superconducting coplanar waveguide resonator by means of the atomlaser scheme. We have shown that by the counting of single atoms outcoupled by the measured field and falling out of the trap due to gravity, weak microwave fields at the single-photon level can be sensed and translated to a detectable signal of a few atoms.

Appendix A: Transitions between the $F = 1$ and $F = 2$ hyperfine manifolds

Transitions between the $F = 2$ and $F = 1$ manifolds of the $5^2S_{1/2}$ ground state of ^{87}Rb are magnetic dipole transitions. As the quantum numbers L and m_L are both zero and the nuclear Landé factor g_I is much smaller than the spin Landé factor g_S, it is the spin magnetic moment $\boldsymbol{\mu}_S = -g_S\mu_B\hat{\mathbf{S}}$ which determines the coupling of the atomic magnetic moment with a resonant, oscillating magnetic field that is orthogonal to the offset field. The x and y components of $\boldsymbol{\mu}_S$ can be expressed by the spin raising and lowering operators $\hat{S}_+ = \hat{S}_x + i\hat{S}_y$ and $\hat{S}_- = \hat{S}_x - i\hat{S}_y$, therefore, it is the nonzero matrix elements of $\hat{S}_+$ and $\hat{S}_-$ which determine the possible transitions. (This can be seen by expressing the basis states $\{|F, m_F\rangle, F = 1, 2, m_F = -F, \ldots, F\}$ common to the operators $\hat{\mathbf{S}}^2, \hat{\mathbf{I}}^2, \hat{\mathbf{F}}^2, \hat{F}_z$ with the basis states $\{|m_S, m_I\rangle, m_S = -1/2, 1/2, m_I = -3/2, \ldots, 3/2\}$ common to the operators $\hat{\mathbf{S}}^2, \hat{\mathbf{I}}^2, \hat{S}_z, \hat{I}_z$.) We focus on the $|2,1\rangle \rightarrow |1,0\rangle$ transition, because the transition matrix element $\langle 1,0|\hat{S}_-|2,1\rangle \approx -\sqrt{3}/2\sqrt{2}$ is the largest possible involving a field-insensitive final state. (We note that if one chooses the state $|1,-1\rangle$ as the trapped state and the $|2,0\rangle$ state as the untrapped one, then the corresponding transition matrix element of the $\hat{S}_+$ operator is a factor of $1/\sqrt{3}$ smaller.)

Appendix B: Outline of the solution of the outcoupling problem

Here we outline the solution to the partial differential equation (1), following the method presented in Ref. [18]. We use the approximation that the mean-field potential $N_0 g_s \Phi_{\mathrm{BEC}}^2(\mathbf{r})$ is negligible compared to the gravitational potential, and consider the resulting inhomogeneous differential equation as a scattering problem, i.e., use the Green's function of the corresponding free problem to determine the outcoupled wave function. The stationary solution of Eq. (1), including the undepleted BEC assumption, is then given by

$$\hat{\Psi}_{|1,0\rangle}(\mathbf{r}, t) = -\hbar\eta e^{i\Delta t} \int d^3\mathbf{r}'' G_+^{3\mathrm{D}}(\mathbf{r}, \mathbf{r}''; -\hbar\Delta)\Phi_{\mathrm{BEC}}(\mathbf{r}'') = i\hbar\eta e^{i\Delta t} F(\mathbf{r}), \tag{7}$$

where $G_+^{3\mathrm{D}}(\mathbf{r}, \mathbf{r}''; -\hbar\Delta)$ is the advanced (outgoing) energy-dependent Green's function (corresponding to the energy $E = -\hbar\Delta$), which can be written as

$$\begin{aligned} G_+^{3\mathrm{D}}(\mathbf{r}, \mathbf{r}''; -\hbar\Delta) = \frac{1}{(2\pi)^2} \int_{-\infty}^{\infty} dk_x \int_{-\infty}^{\infty} dk_z e^{-ik_x(x-x'')} e^{-ik_z(z-z'')} \\ \times G_+^{1\mathrm{D}}\left(y, y''; -\hbar\Delta - \frac{\hbar^2}{2M}\left(k_x^2 + k_z^2\right)\right), \end{aligned} \tag{8}$$

$G_+^{1\mathrm{D}}$ being the Green's function of the 1D free-fall problem

$$\begin{aligned} G_+^{1\mathrm{D}}(y, y''; E) = -\frac{\pi}{Mgl_0^2} \mathrm{Ai}\left(\frac{y + y'' + |y - y''|}{2l_0} - \frac{E}{Mgl_0}\right) \\ \times \mathrm{Ci}\left(\frac{y + y'' - |y - y''|}{2l_0} - \frac{E}{Mgl_0}\right), \end{aligned} \tag{9}$$

and Ci being the complex Airy function $\mathrm{Ci}(x) = \mathrm{Bi}(x) + i\mathrm{Ai}(x)$. In the above expressions $\mathbf{r}''$ refers to the coordinates of the source (i.e., the atomic cloud), k_x and k_z are the wave numbers in the x and z direction, and $l_0 = (\hbar^2/2M^2g)^{1/3}$ is the natural length of the Airy function.

The outcoupled atom density at a position **r** in this monochromatic outcoupling case is

$$N(\mathbf{r}) = \left\langle \hat{\Psi}^{\dagger}_{|1,0\rangle}(\mathbf{r},t)\hat{\Psi}_{|1,0\rangle}(\mathbf{r},t)\right\rangle = (\hbar\eta)^2\left|F(\mathbf{r})\right|^2 = \left(\frac{\hbar\eta}{Mgl_0}\right)^2 D(\mathbf{r}), \tag{10}$$

where

$$D(\mathbf{r}) = (Mgl_0)^2\left|F(\mathbf{r})\right|^2 \tag{11}$$

has the dimension of 1/volume and is dependent on the geometry of the BEC cloud. We note that when the outcoupling magnetic field has a spectral distribution, then $D(\mathbf{r})$ is a function of the frequency, and may be considered the so-called spectral resolution function of the BEC as a measuring device [18].

For coordinates below a spherical BEC with radius a, in the Tomas–Fermi approximation

$$\begin{aligned} F(\mathbf{r}) = &-\frac{\pi}{Mgl_0}\sqrt{\frac{\mu}{Ng_s}}\int_0^{\infty} d\bar{k}_\perp \bar{k}_\perp J_0(\bar{k}_\perp \bar{r}_\perp)\mathrm{Ci}\left(\bar{y} - \frac{E_y(\bar{k}_\perp)}{Mgl_0}\right) \\ &\times \int_0^1 d\bar{r}''_\perp \bar{r}''_\perp J_0\left(\bar{k}_\perp \bar{r}''_\perp\right)\int_{-\bar{a}\sqrt{1-(\bar{r}''_\perp)^2}}^{\bar{a}\sqrt{1-(\bar{r}''_\perp)^2}} d\bar{y}''\sqrt{1-\left(\bar{r}''_\perp\right)^2 - \frac{(\bar{y}'')^2}{\bar{a}^2}} \\ &\times \mathrm{Ai}\left(\bar{y}'' - \frac{E_y(\bar{k}_\perp)}{Mgl_0}\right). \end{aligned} \tag{12}$$

Here $\bar{k}_\perp$ is the length of the dimensionless wave vector perpendicular to the direction of gravity, with $\bar{k}_\perp^2 = a^2(k_x^2 + k_z^2) = 2Ma^2(E_x + E_z)/\hbar^2$, $E_y(\bar{k}_\perp) = -\hbar\Delta - \hbar^2\bar{k}_\perp^2/2Ma^2$, $\bar{r}''_\perp = \sqrt{(x'')^2 + (z'')^2}/a$ is the length of the dimensionless position vector perpendicular to gravity, while $\bar{y}'' = y/a$ is the dimensionless coordinate in the direction of gravity inside the BEC. $\bar{r}_\perp$ refers to the dimensionless length of the position vector **r** perpendicular to gravity [18].

Appendix C: Analytical formulas for the magnetic field of a CPW

If the transverse size of the conductors and their distance is small relative to the mode wavelength of the cavity, then the quasi-static approximation may be applied [26]. Let us introduce the coordinates $x' = x$, $y' = y - d$, $z' = z + L/2$ (see Fig. 1) to describe the magnetic field components of the CPW, where d is the distance between the center of the BEC and that of the CPW. For reasons of symmetry, it suffices to restrict to one half of the structure (i.e., $0 \le x' \le b$, $0 \le z' \le L$), and consider the CPW as coupled slots [27]. We assume magnetic walls at $x' = 0$ and $x' = b = S/2 + W + w$ and open-circuit boundary conditions at $z' = 0$ and $z' = L = \lambda_g/2$, with λ_g being the mode wavelength [27, 28]. As a result of the longitudinal boundary condition, the maxima of the electric and magnetic fields are shifted in space. The magnetic field is maximal at $z' = L/2$, where the electric field is zero, and zero at the two ends, where the electric field is maximal. Here we only present the components of the magnetic field for the case of odd (transverse) excitations, according to Ref. [22]. On the air side of the structure ($y' \le 0$) they can be approximated as

$$B_x(\mathbf{r}') = p\left[\sum_{n>0}^{\infty}\frac{s_n}{F_n}\cos\left(\frac{n\pi x'}{b}\right)e^{-\gamma_n|y'|}\right]\sin\left(\frac{\pi z'}{L}\right),$$

$$B_y(\mathbf{r}') = p\left[\sum_{n>0}^{\infty} s_n \sin\left(\frac{n\pi x'}{b}\right) e^{-\gamma_n |y'|}\right] \sin\left(\frac{\pi z'}{L}\right), \tag{13}$$

$$B_z(\mathbf{r}') = p\frac{2b}{\lambda_g}\left[\sum_{n>0}^{\infty} q\frac{s_n}{nF_n} \sin\left(\frac{n\pi x'}{b}\right) e^{-\gamma_n |y'|}\right] \cos\left(\frac{\pi z'}{L}\right),$$

where

$$p = -i\mu_0\mu_r \frac{4V_0}{\eta b}\frac{\lambda}{\lambda_g}, \tag{14}$$

$$s_n = \frac{\sin(\frac{n\pi\delta}{2})}{\frac{n\pi\delta}{2}} \sin\left(\frac{n\pi\bar{\delta}}{2}\right), \tag{15}$$

$$q = 1 - \left(\frac{\lambda}{\lambda_g}\right)^2, \tag{16}$$

$$F_n = \frac{b\gamma_n}{n\pi} = \sqrt{1 + \left(\frac{2b\nu}{n\lambda}\right)^2}, \tag{17}$$

with $\delta = W/b$, $\bar{\delta} = (S+W)/b$, $\nu = \sqrt{(\lambda/\lambda_g)^2 - 1}$, μ_0 is the permeability of free space, $\mu_r \approx 1$ is the relative permittivity of the conductor, $\eta = \sqrt{\mu_0/\varepsilon_0}$ is the impedance of free space, and V_0 is the voltage directly across the slot between the central and ground electrodes. Let us note that the complex factor i in the expression of p is due to the fact that there is a $\pi/2$ phase difference in the time dependence of the magnetic field and the electric field, i.e., when the magnetic field is maximal in time, then the electric field is zero and vice versa.

For the case when $b \ll \lambda, h$, where h is the thickness of the substrate, it can be shown that the magnetic field on the substrate side of the structure is approximately given by

$$\begin{aligned} B_x^{0\le y'\le h}(x',y',z') &\approx -B_x(x',-y',z'),\\ B_y^{0\le y'\le h}(x',y',z') &\approx B_y(x',-y',z'), \end{aligned} \tag{18}$$

while the z components of the magnetic field can be neglected on both sides of the CPW, i.e., $|B_z(\mathbf{r}')|, |B_z^{0\le y'\le h}(\mathbf{r}')| \ll |B_x(\mathbf{r}')|, |B_y(\mathbf{r}')|$.

Appendix D: Effective dielectric constant and the capacitance of a CPW

For a conventional CPW on a substrate of relative permittivity ε_r, the effective dielectric constant ε_{eff} and the capacitance per unit length c_{CPW} can be analitically approximated using conformal mapping techniques as [22]

$$\varepsilon_{\text{eff}} = 1 + \frac{\varepsilon_r - 1}{2}\frac{\kappa_1}{\kappa_0}, \tag{19}$$

$$c_{\text{CPW}} = 4\varepsilon_0\varepsilon_{\text{eff}}\kappa_0, \tag{20}$$

where $\kappa_i = K(k_i)/K(k_i')$, K being the complete elliptic integral, $k_0 = S/(S+2W)$, $k_1 = \sinh(\frac{\pi S}{4h})/\sinh(\frac{\pi(S+2W)}{4h})$, $k_i' = \sqrt{1-k_i^2}$ for $(i = 0, 1)$.

Acknowledgements
The authors would like to thank Johannes Fink for helpful discussions.

Funding
This work was supported by the National Research, Development and Innovation Office of Hungary (Project Nos. K115624, K124351, PD120975, 2017-1.2.1-NKP-2017-00001). O. K. acknowledges support from the János Bolyai Research Scholarship of the Hungarian Academy of Sciences.

Abbreviations
BEC, Bose–Einstein condensate; CPW, coplanar waveguide resonator; CQED, circuit quantum electrodynamics.

Availability of data and materials
Not applicable.

Competing interests
The authors declare that they have no competing interests.

Authors' contributions
OK performed the calculations. All authors participated in the design and discussion of the setup and the model of the system, and contributed equally to the writing of this paper. All authors read and approved the final manuscript.

Publisher's Note

Received: 30 November 2018 Accepted: 8 January 2020 Published online: 15 January 2020

References

1. Gleyzes S, Kuhr S, Guerlin C, Bernu J, Deléglise S, Busk Hoff U, Brune M, Raimond JM, Haroche S. Quantum jumps of light recording the birth and death of a photon in a cavity. Nature. 2007;446:297–300.
2. Schuster DI, Houck AA, Schreier JA, Wallraff A, Gambetta JM, Blais A, Frunzio L, Majer J, Johnson B, Devoret MH, Girvin SM, Schoelkopf RJ. Resolving photon number states in a superconducting circuit. Nature. 2007;445:515–8.
3. Vijay R, Devoret MH, Siddiqi I. The Josephson bifurcation amplifier. Rev Sci Instrum. 2009;80:111101.
4. Johnson BR, Reed MD, Houck AA, Schuster DI, Bishop LS, Ginossar E, Gambetta JM, DiCarlo L, Frunzio L, Girvin SM, Schoelkopf RJ. Quantum non-demolition detection of single microwave photons in a circuit. Nat Phys. 2010;6:663–7.
5. Inomata K, Lin Z, Koshino K, Oliver WD, Tsai J-S, Yamamoto T, Nakamura Y. Single microwave-photon detector using an artificial Λ-type three-level system. Nat Commun. 2016;7:12303.
6. Kono S, Koshino K, Tabuchi Y, Noguchi A, Nakamura Y. Quantum non-demolition detection of an itinerant microwave photon. Nat Phys. 2018;14:546–9.
7. Besse J-C, Gasparinetti S, Collodo MC, Walter T, Kurpiers P, Pechal M, Eichler C, Wallraff A. Single shot quantum nondemolition detection of individual itinerant microwave photons. Phys Rev X. 2018;8:021003.
8. Girvin SM. Circuit QED: superconducting qubits coupled to microwave photons. In: Devoret M, Huard B, Schoelkopf R, Cugliandolo LF, editors. Quantum machines: measurement and control of engineered quantum systems. Lecture notes of the les houches summer school. vol. 96. Oxford: Oxford University Press; 2011. p. 113–255.
9. Taylor JM, Cappellaro P, Childress L, Jiang L, Budker D, Hemmer PR, Yacoby A, Walsworth R, Lukin MD. High-sensitivity diamond magnetometer with nanoscale resolution. Nat Phys. 2008;4:810.
10. Li PB, Liu YC, Gao SY, Xiang ZL, Rabl P, Xiao YF, Li FL. Hybrid quantum device based on NV centers in diamond nanomechanical resonators plus superconducting waveguide cavities. Phys Rev Appl. 2015;4:044003.
11. Wildermuth S, Hofferberth S, Lesanovsky I, Haller E, Andersson M, Groth S, Bar-Joseph I, Krüger P, Schmiedmayer J. Bose–Einstein condensates: microscopic magnetic-field imaging. Nature. 2005;435:440.
12. Fortágh J, Zimmermann C. Magnetic microtraps for ultracold atoms. Rev Mod Phys. 2007;79(1):235–89.
13. Folman R, Krüger P, Denschlag J, Henkel C, Schmiedmayer J. Microscopic atom optics: from wires to an atom chip. Adv At Mol Opt Phys. 2002;48:263–356.
14. Öttl A, Ritter S, Köhl M, Esslinger T. Correlations and counting statistics of an atom laser. Phys Rev Lett. 2005;95:090404.
15. Köhl M, Öttl A, Ritter S, Donner T, Bourdel T, Esslinger T. Time interval distributions of atoms in atomic beams. Appl Phys B. 2007;86:391–3.
16. Kálmán O, Kiss T, Fortágh J, Domokos P. Quantum galvanometer by interfacing a vibrating nanowire and cold atoms. Nano Lett. 2012;12(1):435–9.
17. Federsel P, Rogulj C, Menold T, Fortágh J, Günther A. Spectral response of magnetically trapped Bose gases to weak microwave fields. Phys Rev A. 2015;92:033601.
18. Kálmán O, Darázs Z, Brennecke F, Domokos P. Magnetic-noise-spectrum measurement by an atom laser in gravity. Phys Rev A. 2016;94:033626.
19. Verdú J, Zoubi H, Koller C, Majer J, Ritsch H, Schmiedmayer J. Strong magnetic coupling of an ultracold gas to a superconducting waveguide cavity. Phys Rev Lett. 2009;103:043603.
20. Hattermann H, Bothner D, Ley LY, Ferdinand B, Wiedmaier D, Sárkány L, Kleiner R, Koelle D, Fortágh J. Coupling ultracold atoms to a superconducting coplanar waveguide resonator. Nat Commun. 2017;8:2254.
21. Stibor A, Bender H, Kühnhold S, Fortágh J, Zimmermann C, Günther A. Single-atom detection on a chip: from realization to application. New J Phys. 2010;12:065034.
22. Simons RN. Coplanar waveguide circuits, components, and systems. New York: Wiley; 2001.
23. Schneeweiss P, Gierling M, Visanescu G, Kern D, Judd T, Günther A, Fortágh J. Dispersion forces between ultracold atoms and a carbon nanotube. Nat Nanotechnol. 2012;7:515.

24. Jetter B, Märkle J, Schneeweiss P, Gierling M, Scheel S, Günther A, Fortágh J, Judd T. Scattering and absorption of ultracold atoms by nanotubes. New J Phys. 2013;15:073009.
25. Megrant A, Neill C, Barends R, Chiaro B, Chen Y, Feigl L, Kelly J, Lucero E, Mariantoni M, O'Malley PJJ, Sank D, Vainsencher A, Wenner J, White TC, Yin Y, Zhao J, Palmstrøm CJ, Martinis JM, Cleland AN. Planar superconducting resonators with internal quality factors above one million. Appl Phys Lett. 2012;100:113510.
26. Pozar DM. Microwave engineering. Hoboken: Wiley; 2011.
27. Knorr JB, Kuchler KD. Analysis of coupled slots and coplanar strips on dielectric substrate. IEEE Trans Microw Theory Tech. 1975;23(7):541–8.
28. Simons RN. Suspended coupled slotline using double layer dielectric. IEEE Trans Microw Theory Tech. 1981;29(2):162–5.